Journal of Chromatography A, 1217 (2010) 1604–1615

Contents lists available at ScienceDirect

Journal of Chromatography A

journal homepage: www.elsevier.com/locate/chroma

Performance of columns packed with the new shell Kinetex-C_{18} particles in gradient elution chromatography

Fabrice Gritti, Georges Guiochon*

Department of Chemistry, University of Tennessee, Knoxville, TN 37996-1600, USA

ARTICLE INFO

Article history:
Received 25 October 2009
Received in revised form 2 December 2009
Accepted 6 January 2010
Available online 18 January 2010

Keywords:
Column packing technology
Shell particles
Gradient elution
Peak capacity
Kinetex-C_{18}
Halo-C_{18}
BEH-C_{18}
β-Lactoglobulin
Protein digest
Bradykinin
Insulin
Lyzozyme
Acetonitrile

ABSTRACT

The performance of columns packed with the new 2.6 μm Kinetex-C_{18} shell particles was investigated in gradient elution chromatography and compared with those of the 2.7 μm Halo-C_{18} shell particles and the 1.7 μm BEH-C_{18} totally porous particles. The peak capacities P_c of these columns were derived from the resolution of the components of a peptide mixture (β-Lactoglobulin digest) and of a mixture of two biomolecules (insulin and lyzozyme).The three columns exhibit the same peak capacities for the peptides at low linear velocity ($u_0 < 0.05$ cm/s) and at any gradient steepness ($0.8 < G < 10$). When the linear velocity is increased 10-fold, the peak capacity of the Kinetex column remains nearly unchanged while those of the Halo-C_{18} and the BEH-C_{18} columns decrease by 20%, approximately. This result confirms the very flat HETP curve, the very low C term of the Kinetex column and its ability to successfully operate at high flow rates while experiencing less efficiency loss than other columns. Despite its smaller average mesopore size (96 Å *versus* 130 Å), the column packed with 2.6 μm shell Kinetex-C_{18} particles gives an equivalent or even slightly better separation of biomolecules having a size and a mass around 40 Å and 15 kDa, respectively, than the column packed with 1.7 μm BEH-C_{18} totally porous particles. This result demonstrates the advantages of the shell *versus* the conventional particle technology when it comes to resolve mixtures of large and slow diffusive biomolecules.

1. Introduction

The rapid evolution of packed column technology over the last 10 years was marked by the successive appearance of the silica monolithic rods [1–3], the sub-2 μm particles [4,5], and the shell particles [6–9]. Currently, efficiencies of more than 100,000 plates per meter can consistently be achieved by monolithic columns [10] while efficiencies of at least 300,000 plates per meter are readily achieved with columns packed with sub-2 μm particles, with only a small efficiency loss due to heat friction and to the formation of radial temperature gradient when these columns are operated under nearly adiabatic conditions [11]. In both cases and for different reasons (the extremely high permeability of monolithic columns and the small hold-up volume of sub-2 μm particle packed columns), analysis times were reduced by nearly an order of magnitude compared to those achieved with columns packed with conventional 5 μm particles, which dominated the field one decade ago. Nevertheless, serious difficulties remain. The acceptance by the analyst community of columns packed of sub-2 μm particles is hampered by the heavy cost required to switch from conventional HPLC systems (which can operate at a maximum inlet pressure of 400 bar) to chromatographs of the new generation that are able to operate at inlet pressures up to 1200 bar. Conversely, the efficiency of the monolithic columns that are now available is low, due to their radial heterogeneity. Progress would require either improved column manufacturing or the development of a dedicated injection procedure placing the sample at the very center of the monolithic rod, where its bed is homogeneous [10]. However, such improvements come but slowly.

In order to overcome the limitations of the sub-2 μm particles and of monolithic silica rods, some manufacturers have focused on the development of very efficient columns that could supply separations exhibiting minimum plate heights around 3 μm (i.e., efficiencies in excess of 300,000 plates per meter) with a specific permeability comparable to that of columns packed with 3 μm particles ($k_0 \simeq 9 \times 10^{-11}$ cm^2). These columns would deliver analyses comparable to those achieved with the best columns packed with sub-2 μm particles but could be operated with the same instruments as those used for conventional columns. At the same time, these manufacturers propose adjustments of the injection/connector/detection systems of conventional HPLC instruments that would minimize the contributions to band

* Corresponding author. Fax: +1 865 974 2667.
E-mail address: guiochon@utk.edu (G. Guiochon).

0021-9673/$ – see front matter © 2010 Elsevier B.V. All rights reserved.
doi:10.1016/j.chroma.2010.01.008

broadening due to the extra-column volumes of the instruments. These contributions that have negligible influence on the effective efficiency of conventional columns cause an excessive decrease of the intrinsic performance of highly efficient columns [12]. This last aspect of column technology is suddenly becoming very important because the ability of using the most advanced columns on conventional instruments permits large savings.

To keep the column back-pressures moderate (i.e., below 400 bar) and still operate columns at velocities significantly larger than the optimum velocity for maximum column efficiency, the particle size should range between 2.5 and 3.0 μm [7]. In order to improve the column efficiency, researchers have focused on the development of either shell or superficially porous particles. In theory, decreasing the thickness of the porous layer of porous material should cause a decrease of the *C* term in the van Deemter plot, because the length along which molecules should diffuse decreases [13]. First, Advanced Material Technology, ended up with the 2.7 μm superficially porous or shell Halo-C_{18} particles [6,7,14–17]. This exceptionally performing material was made of 1.7 μm solid silica core covered by a 0.5 μm porous silica shell. It provided minimum reduced HETPs of ca. 1.4±0.17 for low molecular weight compounds [18], a significant improvement in packed column technology since the minimum reduced HETP of totally porous particle is usually of the order of 2.2. More recently, Phenomenex developed columns packed with a new type of shell particle (2.6 μm Kinetex particles) that are made of a 1.9 μm solid silica core and a 0.35 μm thick layer of porous silica. The lowest value of the reduced HETP measured on this column was only 1.15 ± 0.14 for the low molecular weight anthracene in pure acetonitrile [12], an unprecedented record in HPLC column technology. Most strikingly, the *C* term or overall coefficient of mass transfer resistance between mobile and stationary phases measured for a Kinetex-C_{18} column for compounds having low diffusion coefficients, like insulin and lyzozyme, was nearly eight times smaller than for the Halo-C_{18} column. No definitive reason has yet been suggested to explain such a large difference between the performance of columns packed with these two particles, except the difference in the roughness of the external surface and the porosity of the shell of these two particles.

Besides their structure, made of a shell around a solid core particle, the interesting feature of these superficially porous particles is their extremely narrow size distribution (PSD). Their $d_{90/10}$ size ratio is typically 1.13 ± 0.02 [12] while it is usually within the range between 1.5 and 2.0 for conventional totally porous particles. This characteristic feature of shell particles was unexpected; it is not understood why building porous shells would eventually lead to extremely narrow PSDs, unless the production process of solid core particles leads readily to a narrow PSD. It is suspected that this narrow PSD is the key for their success at separating small molecules [6,7,14], although the rational behind this assertion is unclear. It is inconsistent with previous experimental results [19]. Carta and Bauer [20] calculated elution profiles for columns having beds made of particles of the same average size but different size distributions. They showed that, if the distribution was symmetrical, its variance had little influence on the profile. Strongly skewed distributions only may affect elution profiles. Recent measurements have shown that columns packed with shell particles are not more radially homogeneous than those packed with traditional totally porous particles [21]. This suggests that the higher performance of columns packed with shell particles does not result from a decrease of their transcolumn structure heterogeneity. The exceptionally low reduced HETPs measured with shell particles seems to be better explained by a diminution of their short-range interchannel velocity biases, biases that take place over average distances of one particle diameter [12]. Additional measurements of the transcolumn velocity biases in the Kinetex column are needed in order to assess its contribution to the eddy dispersion term in the Kinetex column.

The goal of this work is a further characterization of the kinetic performance of columns packed with Kinetex-C_{18} shell particles, in the gradient elution mode. For a sake of a comparison with some of the best performing conventional columns available, we measured and compared the peak capacities for mixtures of peptides and proteins of three high performance columns: (1) a 100 mm × 4.6 mm column packed with 2.6 μm Kinetex-C_{18} shell particles; (2) a 150 mm × 4.6 mm column packed with 2.7 μm Halo-C_{18} particles; and (3) a 100 mm × 3.0 mm column packed with 1.7 μm BEH-C_{18}. The peak capacities were measured with the same samples on each column, at constant chromatographic linear velocity and intrinsic gradient steepness, in order to generate comparable retention windows for the least and the most retained compounds. A model accounting for the compression factor in gradient elution is used to predict the experimental peak capacity and serve as a reference for the comparison between the performance of the three columns [22,23].

2. Theory

2.1. Theoretical peak capacity

The definition and the general expression of the peak capacity P_c in chromatography, assuming a resolution of unity between the successively eluted peaks is written [24]:

$$P_c = 1 + \int_{t_I}^{t_F} \frac{1}{4\sigma} dt \tag{1}$$

where t_I is the retention time of the first eluted peak (usually that of a non-retained compound), t_F is the retention time of the last eluted peak, dt is a dummy time variable, and σ is the time standard deviation of a peak.

In this work, we assume that the plate height H of the column remains independent of the mobile phase composition. Accordingly, the time band variance σ of an eluted peak is [25]:

$$\sigma^2 = G_{12}^2 HL \left(\frac{1 + k'_E}{u_0} \right)^2 \tag{2}$$

where u_0 is the chromatographic linear chromatographic velocity (related to the hold-up time t_0), k'_E is the retention factor of the sample at the column outlet, L is the column length, and G_{12}^2 is the band compression factor. With the linear solvent strength (LSS) retention model and for linear, non-retained, and non-distorted gradients, the band compression factor was derived by Poppe et al. [26]:

$$G_{12}^2 = \frac{1 + p + (1/3)p^2}{(1+p)^2} \tag{3}$$

where p is defined as [26]:

$$p = S \frac{\Delta\varphi}{t_g} t_0 \frac{k'_0}{1 + k'_0} = G \frac{k'_0}{1 + k'_0} \tag{4}$$

where $\Delta\varphi$ is the change in solvent composition during the gradient, t_g is the gradient run time (with $\beta = \Delta\varphi / t_g$ the gradient slope), t_0 is the column hold-up time, S is the slope of the relationship between the natural logarithm of the retention factor measured under isocratic conditions and the organic solvent concentration in the case of the LSS model, k'_0 is the retention factor of the compound at the beginning of the gradient, and $G = S\beta t_0$ is the intrinsic gradient steepness [27]. The LSS model is written [27]:

$$\ln k' = \ln k'_0 - S(\varphi - \varphi_0) \tag{5}$$

where φ_0 is the volumetric fraction of the strong eluent at the beginning of the gradient.

For linear, non-retained, and non-distorted gradients, we can calculate exactly the mobile phase composition $\varphi(t, z)$ at any time t and any position z inside the column:

$$\varphi(t,z) = \varphi_0 + \beta\left(t - \frac{z}{u_0}\right) \quad (6)$$

In Eq. (1), the dummy variable t can be changed to the dimensionless variable k as [24]:

$$k = \frac{t - t_0}{t_0} = \frac{u_0 t}{L} - 1 \quad (7)$$

The variable k is similar to a retention factor and can be derived from the elution time t of a compound. Note that k has nothing to do with the actual retention factor of the same compound at the column outlet, k'_E. Differentiating Eq. (7) gives:

$$dt = \frac{L}{u_0} dk \quad (8)$$

The dummy variable k can be expressed as a function of the intrinsic gradient steepness G and the initial retention factor k'_0 from the expression of the elution time t of a compound in linear gradient elution, assuming a LSS retention model and a linear, non-retained, and non-distorted gradient. Accordingly, k is written [27]:

$$k = \frac{t - t_0}{t_0} = \frac{1}{G}\ln\left(1 + Gk'_0\right) \quad (9)$$

Eq. (9) provides a direct relationship between the initial retention factor k'_0, the dummy variable k, and the intrinsic gradient steepness G:

$$k'_0 = \frac{1}{G}\left(e^{Gk} - 1\right) \quad (10)$$

Note that, in this model, we assumed constant the intrinsic gradient steepness G. Substituting Eq. (10) into Eq. (4) provides an explicit relationship between the band compression parameter p and the variable k:

$$p = G\frac{e^{Gk} - 1}{G + e^{Gk} - 1} \quad (11)$$

The retention factor at the column outlet k'_E is obtained from Eqs. (5), (6), and (9) at $z = L$ and at the time t corresponding to the elution of the peak. Accordingly,

$$k'_E = \frac{k'_0}{1 + Gk'_0} \quad (12)$$

Combining Eqs. (10) and (12), gives the following explicit relationship between k'_E and k:

$$k'_E = \frac{1}{G}\frac{e^{Gk} - 1}{e^{Gk}} \quad (13)$$

Finally, after integration and simplification, Eq. (1) and the theoretical peak capacity become

$$P_c = 1 + \frac{1}{4}\sqrt{\frac{3L}{\omega H}}\ln\left[\frac{2\omega e^{Gk_F} + G^2 - 6 + \psi}{G(2\sqrt{3\omega} + 3G + 6)}\right] \quad (14)$$

where

$$\omega = G^2 + 3G + 3 \quad (15)$$

$$\psi = 2\sqrt{\omega\left[(G^2 - 6)e^{Gk_F} + \omega e^{2Gk_F} + G^2 - 3G + 3\right]} \quad (16)$$

$$k_F = \frac{t_F - t_0}{t_0} = \frac{1}{G_8}\ln\left(1 + G_8 k'_{0,8}\right) \quad (17)$$

In Eq. (17), $G_8 = S_8\beta t_0$ and $k'_{0,8}$ are the intrinsic gradient steepness and retention factor at the beginning of the gradient, measured of the last eluted compound (peak labeled as #8 in Figs. 2–4). These parameters are directly measured from the elution times of this compound for three different gradient slopes β.

The theoretical peak capacity (Eq. (14)) is an explicit function of the width of the retention window (k_F), assuming that the column HETP H remains constant, is the same for all components and all mobile phase compositions, all column lengths L, and all intrinsic gradient steepness G. Rigorously, G depends on the parameter S which *a priori* differs from one peptide to another and from one column to another. For instance, we measured values of 28 and 25 for the S parameter of the peak labeled #6, values of 33 and 29 for bradykinin, of 66 and 67 for insulin, and of 100 and 89 for lyzozyme on the Kinetex and the BEH columns, respectively. It seems that the values of the S parameters are at most + 15% larger for the shell particles than for the fully porous ones. At constant H (column efficiency), constant L (column length) and constant k_F (gradient window), Eq. (14) predicts a increase of the peak capacity from 2 to 7% as G increases by 15% within the range of G =1–9. In the same time, decreasing H by 15% results in an increase of the peak capacity of 9%. Since the S values are slightly larger with the Kinetex column than with the BEH column, the experimental peak capacity of the BEH column should be increased from 2 to 7% to get a fair comparison. Similar remarks can be made for differences in column lengths. For instance, increasing the column length from 10 to 15 cm and keeping everything else constant, would lead to an increase of the peak capacity of 6% for G =1.25, and a decrease of the peak capacity of −4% and −10% for G =3.8 and 11.4, respectively. In conclusion, the effect of the column length is not straightforward nor very important in gradient elution chromatography.

For the sake of simplicity, we assumed a constant value of S for the derivation of equation Eq. (14). This assumption, which makes the calculations possible, is reasonable when the size and the concentration distributions of the sample components are as narrow as they are for protein digests [28]. Accordingly, for each column, S was taken as the arithmetic average of the S_i values measured for the three selected peptides, which are eluted at the beginning, in the center, and at the end of the retention window (peaks labeled 2, 6, and 8 in Figs. 2–4). The S_i values were estimated by minimizing the distance between the experimental elution time of each peak for three known gradient slopes β and the theoretical ones assuming Eq. (9). Finally, the agreement between experimental (see next section) and theoretical peak capacities allows the derivation of an estimate of a constant H for each column, which will serve as an indicator of the column performance in gradient elution. This value of H will be compared to the average particle diameter d_p. The smaller the ratio H/d_p, the better the column performance in gradient elution.

2.2. Experimental peak capacity

The experimental peak capacity was estimated according to [24]:

$$P = 1 + \frac{t_N - t_1}{(1/N)\sum_{i=1}^{i=N}\omega_i} \quad (18)$$

where t_N and t_1 are the gradient elution times of the most and less retained peak, respectively, N is the number of peaks selected for the calculation, and ω_i is the baseline peakwidth of the i^{th} selected peak. ω_i was measured as follows [29]:

$$\omega_i = \frac{2(t_{1/2,r,i} - t_{1/2,f,i})}{\sqrt{1.38629}} \quad (19)$$

where $t_{1/2,r,i}$ and $t_{1/2,f,i}$ are the experimental elution times of the rear and front parts of the peak measured at half its height.

The selection of the peaks was only based on their heights, in order to minimize the errors made in the measurement of their widths. So, it is possible that changing the gradient steepness could induce some changes in the elution order of these peaks. However, the evolution of the widths of the peaks of the eight selected compounds from one gradient steepness to the other remains parallel, meaning that the probability of peak misidentification from one gradient steepness to another is small.

3. Experimental

3.1. Chemicals

The mobile phase used in this work was made of a mixture of water, acetonitrile, and trifluoroacetic acid (TFA). Dichloromethane ($\rho_{CH_2Cl_2}$=1.306 g/cm^3) and isopropanol (ρ_{iPrOH}=0.782 g/cm^3) were used in small amounts, to measure the hold-up times t_0 of the columns by pycnometry. All solvents were HPLC grade from Fisher Scientific (Fair Lawn, NJ, USA). The mobile phase was filtered before use on a surfactant-free cellulose acetate filter membrane, 0.2 μm pore size (Suwannee, GA, USA). Thiourea, trifluoro acetic acid, and lyzozyme were purchased from Aldrich (Milwaukee, WI, USA). bradykinin was from American Peptides Company Inc. (Sunnyvale, CA). Insulin was a generous gift from Eli Lilly (Indianapolis, IN, USA). The β-lactoglobulin protein digest was obtained from an in-solution digestion protocol detailed in [30].

3.2. Columns

The new Kinetex-C$_{18}$ column (100 mm ×4.6 mm) was a generous gift from the column manufacturer (Phenomenex, Torrance, CA, USA). The Halo-C$_{18}$ column (150 mm ×4.6 mm) was purchased from Advanced Material Technology (Wilmington, DE, USA). The BEH-C$_{18}$ column (100 mm × 3.0 mm) was a gift from Waters (Milford, MA, USA). The main characteristics of the bare porous silica and those of the final derivatized packing material are summarized in Table 1.

3.3. Apparatus

The gradient elution data were acquired with an Acquity UPLC (Waters, Milford, MA, USA) liquid chromatograph. This instrument includes a quaternary solvent delivery system, an auto-sampler with a nominal 5 μL sample loop, actually calibrated at 7.1 μL by the instrument calibration measurement. The injection volume was set at 5 μL with partial loop with needle overfill as the sample loop option. The instrument is also equipped with a monochromatic UV detector (0.5 μL, sampling rate set at 40 Hz), a column oven, and a data station running the Empower data software from Waters. From the exit of the Rheodyne injection valve to the column inlet and from the column outlet to the detector cell, the total extra-column volume of the instrument is 15.6 μL, measured as the apparent hold-up volume of a zero-volume union connector in place of the column.

The contribution of the injection/connecting tubes/detection system to the peak variance is 8 μL^2 when injecting a 5 μL sample at a flow rate of 0.5 mL/min [12]. In gradient elution mode, due to the sample concentration that takes place at the inlet of the column (most components have large k'_0 values), only the contribution of the detector and the connecting tube between the column outlet and the detector cell contribute to broaden the peak width. This contribution to the peak variance is smaller than 1 μL^2 at a flow rate of 2 mL/min [23]. The smallest recorded peak variances at 2 mL/min are 21 μL^2 for a peptide of the β-lactoglobulin digest, 22 μL^2 for insulin, and 52 μL^2 for lyzozyme. The contribution of the extra-column volumes to the peak variance in gradient elution is thus negligible (<5%).

In order to connect correctly the Halo and the Kinetex columns to the column stabilizer of the Acquity instrument, an additional inlet capillary tube of negligible volume (1.2 μL) and a Acquity union connector were used. The BEH column fits directly to the ferrule and the golden nut at the end of the column stabilizer.

A time offset of 0.71 s was measured after the zero injection time was recorded. The maximum flow rate and pressure that can be applied during an acquisition run are 2.0 mL/min and 732 bar, respectively. The flow rate accuracy was determined by directly pumping the pure mobile phase at 22 °C and 1 mL/min during 50 min into a volumetric flask of 50 mL. The relative error was less

Table 1
Physico-chemical properties of the Kinetex-C$_{18}$, BEH-C$_{18}$, and Halo-C$_{18}$ columns given by the manufacturer and measured in our laboratory [a], [b], [c].

Neat silica	Halo	Kinetex [12]	BEH
Particle size (μm)	2.7	2.5	1.7
$\rho = R_i/R_e$	0.63	0.73	0
Pore diameter (Å)	90	96	130
Surface area (m^2/g)	127	100	185
Particle size distribution ($d_{90-10\%}$)	1.14	1.12	1.59

	Halo-C$_{18}$	Kinetex-C$_{18}$	BEH-C$_{18}$
Bonded phase analysis			
Total carbon (%)	7.5	6	18
Surface coverage (μmol/m^2)	4.0 (C$_{18}$ + endcapping agent)	2.7 (C$_{18}$ only)	3.10
Endcapping	Yes	Yes	Yes
Packed columns analysis			
Lot number/serial number	AH092221/USFH002149	5569-76/496449	01672902130F03
Dimension (mm × mm)	4.6 × 150	4.6 × 100	3.0 × 100
External porosity [a]	0.391	0.372	0.381
Total porosity [b]	0.532	0.542	0.654
Particle porosity	0.232	0.271	0.436
Shell porosity	0.309	0.444	0.436 (totally porous)
Average particle size [c] (K_c = 180)	2.70	2.48	1.86
Specific permeability, k_0 [c] (cm^2)	6.53 × 10^{-11}	4.46 × 10^{-11}	2.77 × 10^{-11}

[a] Measured by Inverse Size Exclusion Chromatography (polystyrene standards).
[b] Measured by pycnometry (iPrOH-CH_2Cl_2).
[c] Measured from the column back pressure data corrected for extra-column contributions and the Kozeny–Carman equation (K_c = 180) from Ref. [12] and from F. Gritti, G. Guiochon, Performance of new prototype packed columns for very-high pressure liquid chromatography, J. Chromatogr. A, in press.

Table 2
Experimental flow rates F_v, gradient times t_g, and intrinsic gradient steepnesses $G(S{\sim}28)$ applied on the Kinetex, Halo, and BEH columns for the analysis of the protein digest (β-lactoglobulin). The increase in the concentration of acetonitrile is maintained constant at $\Delta\varphi = 0.40$ from $\varphi = 0.05$ to 0.45. $H_{peptides}$ is the average column plate height which allows matching experimental and theoretical peak capacities (Eq. (14)).

Column	F_v (mL/min)	u_0 (cm/s)	t_g (min)	$G = S\beta t_{0peptides}$	$H_{peptides}$ (μm)	$H_{peptides}/d_p$
	0.200	0.037	63.0	0.84	8.4	3.2
			21.0	2.53	10.2	3.9
			7.0	7.58	11.7	4.5
Kinetex-C_{18} 100 mm × 4.6 mm	1.000	0.185	12.6	0.84	7.0	2.7
			4.2	2.53	8.7	3.3
			1.4	7.58	10.0	3.8
	2.000	0.370	6.3	0.84	8.1	3.1
			2.1	2.53	10.0	3.8
			0.7	7.58	11.4	4.4
	0.196	0.037	63.0	1.07	7.2	2.7
			21.0	3.22	8.2	3.0
			7.0	9.67	11.4	4.2
Halo-C_{18} 150 mm × 4.6 mm	0.982	0.185	12.6	1.07	6.6	2.4
			4.2	3.22	8.3	3.1
			1.4	9.65	15.4	5.7
	1.963	0.370	6.3	1.07	8.5	3.1
			2.1	3.22	10.1	3.7
			0.7	9.65	17.4	6.4
	0.103	0.037	63.0	0.80	8.4	4.9
			21.0	2.40	11.2	6.6
			7.0	7.21	13.3	7.8
BEH-C_{18} 100 mm × 3.0 mm	0.513	0.185	12.6	0.80	8.8	5.2
			4.2	2.40	12.5	7.4
			1.4	7.21	16.5	9.7
	1.026	0.370	6.3	0.80	13.6	8.0
			2.1	2.40	19.3	11.4
			0.7	7.21	20.5	12.1

than 0.4% (HP1090) and 0.2% (Acquity UPLC), so we estimate the long-term accuracy of the flow-rate at 4 μL/min and slightly better at flow rates around 1 mL/min. The laboratory temperature was controlled by an air conditioning system set at 295 K. The daily variation of the ambient temperature never exceeded ±1 °C.

3.4. Gradient elution experiments

The protein digest (5 μL injection) was eluted under gradient conditions at three different chromatographic linear velocities ($u_0 = L/t_0$ = 0.037, 0.185, and 0.370 cm/s) for each column. The volume fractions of acetonitrile at the beginning and at the end of the gradient were set constant at 5 and 45%, respectively ($\Delta\varphi$=0.40). The concentrations of each component of the sample were unknown. For each linear velocity, three different gradient times t_g were applied in order to allow a direct comparison of the peak capacity P_c between the three columns at constant gradient analysis time. The chromatograms were recorded at a wavelength of 205 nm. This comparison is very practical for analysts. However, we need to keep in mind that the intrinsic gradient steepness G is 1.5 times larger on the Halo column than on either the Kinetex or the BEH columns because the length of the Halo column is 1.5 times that of the other two columns. In the following discussion, according to Eq. (14), we discuss the corrections made to the experimental peak capacity of the Halo column in order to compare the performance of the three columns at the same gradient steepness. However, as explained in the Theory Section, it is difficult to compare different brands of columns for strictly the same gradient steepness because the retention parameter S, hence the retention pattern is likely to vary from one column to the next. Overall, the relative difference in S values is no more than 15% for all the compounds studied in this work and the impact of the variations of S on the peak capacity is less than 7%. In conclusion, any difference in the experimental peak capacity larger than 10% from one column to the next can be considered as significant. Table 2 summarizes the experimental flow rates and gradient times. The corresponding values of the intrinsic gradient steepnesses G are also provided in Table 2.

Similar experimental conditions were applied for the gradient elution of the mixture of thiourea, bradykynin, insulin, and lyzozyme. The sample concentrations were 0.2 g/L for both insulin and lyzozyme. The volume fractions of acetonitrile at the beginning and at the end of gradient were set at 10 and 45%, respectively ($\Delta\varphi$=0.35). Two complementary experimental chromatographic linear velocities were added (u_0=0.0925 and 0.2775 cm/s).

3.5. Measurement of the peak capacity

The experimental determination was based on the measurement of the peak widths of eight different peptides dispersed across the gradient retention window. The peak width was taken as four times the standard deviation σ of each measurable gaussian peak with respect to Eq. (1). For the sake of the accuracy and precision of the measurements of the peak capacities, the eight peaks were selected as having the highest heights. Figs. 2–4 show their respective position in the retention window.

4. Results and discussion

We first discuss and compare the performance of the Kinetex-C_{18}, Halo-C_{18}, and BEH-C_{18} columns with respect to their resolution power of the β-lactoglobulin (mass 18.4 kDa) digest. This sample contains at least 150 peptide residues, based on a manual peak count. In a second part, we focus on the capacity of these columns to separate compounds with larger molecular size, such as globular proteins (5.8 kDa insulin and 13.4 kDa lyzozyme). In both parts, we compare the experimental peak capacities measured on each column. In this work, we deliberately compare the performance of the columns at a constant linear velocity u_0 and at a constant width of their retention window, e.g. at constant gradient slope $\beta = \Delta\varphi/t_g$ The retention window is the time elapsed from the elution of the first component to that of the last one. In addition, for

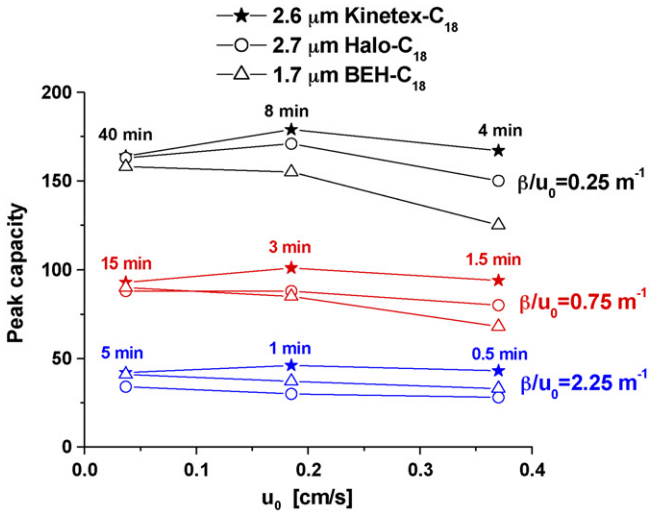

Fig. 1. Peak capacity measured from the resolution of β-lactoglobulin digest as a function of the linear chromatographic velocity u_0. Three column were tested: 100 mm × 4.6 mm 2.6 μm Kinetex shell particles (shell thickness 0.35 μm), 150 mm × 4.6 mm 2.7 μm Halo shell particles (shell thickness 0.50 μm), and 100 mm × 3.0 mm 1.7 μm BEH totally porous particles. Three chromatographic linear velocities u_0 were applied: 0.037, 0.185, and 0.370 cm/s. Three gradient slopes β/u_0 were set for each column and each linear velocity: 0.25, 0.75, and 2.25 m^{-1}. The times given in minute are the retention windows or the difference between the elution times of the selected peptides 8 and 1 (see Fig. 2). Note the constancy of the peak capacity of Kinetex as the flow rate in increased.

a given column, the intrinsic gradient steepness G was kept constant regardless of the flow rate, which allows to measure the sole impact of the flow rate on the quality of the gradient separation.

4.1. Peak capacity for a complex mixture of peptides: β-lactoglobulin digest

A total of 3 × 3 × 3 = 27 chromatograms were recorded, corresponding to three different linear velocities, three different gradient slopes, and three different columns. Fig. 1 collects all the peak capacity data. The columns are represented by different symbols (full stars: Kinetex-C_{18}, empty circles: Halo-C_{18}, and empty triangles: BEH-C_{18}). The times indicated in the graph indicate the retention window of the gradient runs or duration between the elution of the first (1) and last (8) selected peptides. The positions of these peptides are shown in Figs. 2–4, which report the chromatograms recorded with the three columns at the slowest linear velocity u_0=0.037 cm/s, for the three different gradient slopes, β/u_0=0.25, 0.75, and 2.25 m^{-1} in Figs. 2A–C, 3A–C, and 4A–C, respectively. The three gradient slopes are given on the right side of the graph in Fig. 1.

In theory (see Eq. (14)), the peak capacity P_c of a given column should remain constant, independently of the linear velocity, provided that the intrinsic gradient steepness G and the plate height HETP, H, remain constant. Because we deliberately maintained constant the intrinsic gradient steepness G, any significant deviation of the peak capacity from an horizontal line should be due to the effect of the linear velocity on the column plate height of the peptide residues. Actually, the experimental results suggest that the column HETP of the Kinetex and the Halo columns are maximum at an intermediate linear velocity, which is around 0.185 cm/s. The HETP of the peptides is minimum in this range of linear chromatographic velocities. Similar results are expected with small molecules and they should reflect the sole impact of the flow rate on the HETP of the analytes. However, a different trend is observed for the peak capacity of the BEH column, which decreases continuously with increasing linear velocity. This new phenomenon is possibly

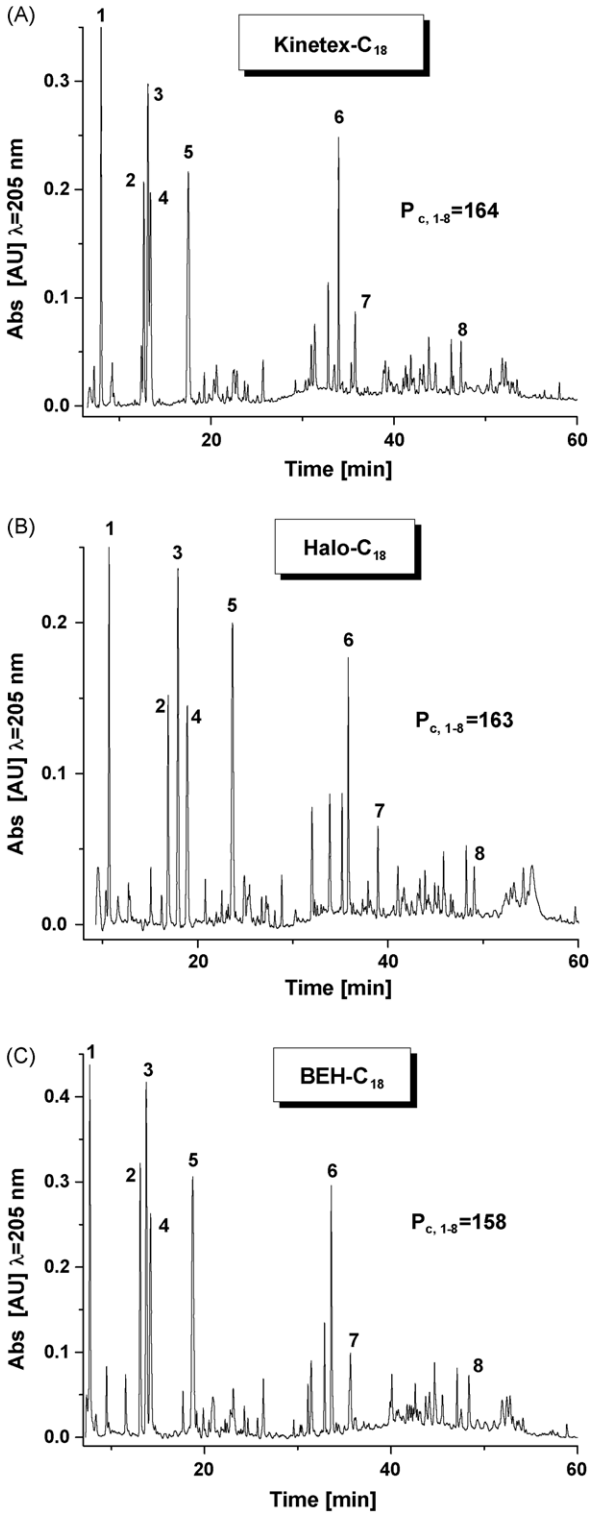

Fig. 2. Chromatograms obtained after the injection of 5 μL of β-lactoglobulin digest in gradient elution. The concentration of acetonitrile at the beginning and at the end of the gradient is equal to 5% and 45%, respectively. The flow rate was set so that the linear velocity u_0 was constant for all three columns at 0.037 cm/s. The gradient slope is maintained constant at β/u_0=0.25 m^{-1}. The numbers in each graph (1–8) locates the eight selected peptides for the estimation of the experimental peak capacity from Eq. (18). The retention window ($t_8 - t_1$) is about 40 min. T = 295 K. (A) 100 mm × 4.6 mm 2.6 μm Kinetex-C_{18} column, (B) 150 mm × 4.6 mm 2.7 μm Halo-C_{18} column, and (C) 100 mm × 3.0 mm 1.7 μm BEH-C_{18} column.

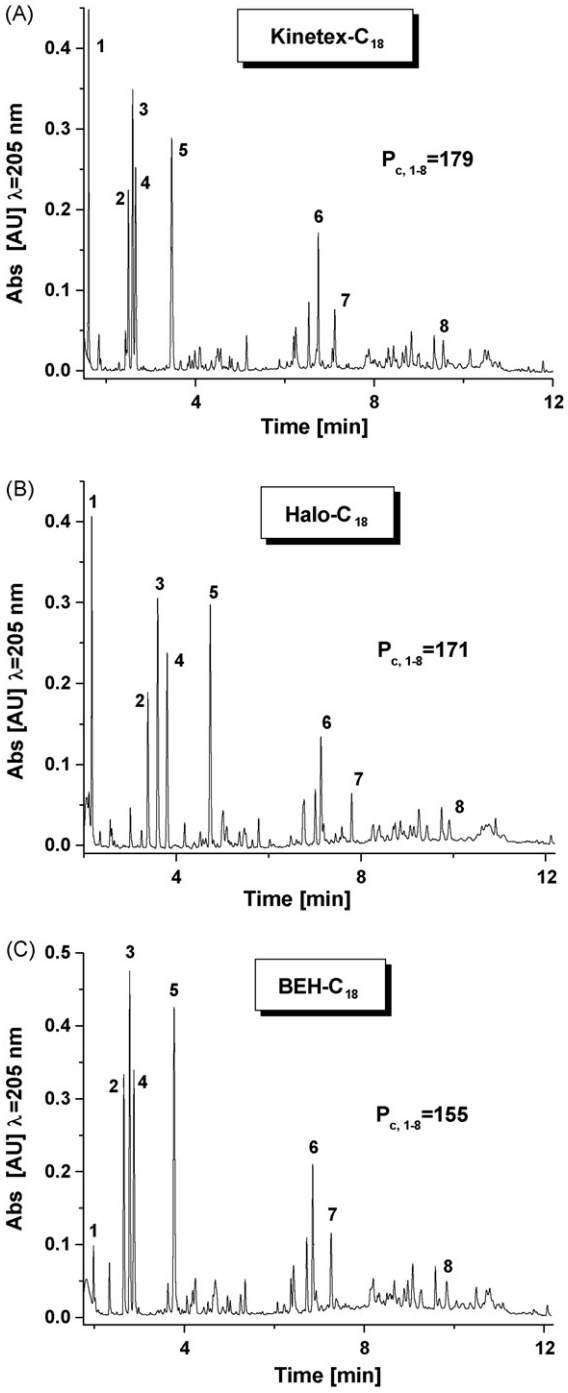

Fig. 3. Same as in Fig. 2 except the linear velocity was set at 0.185 cm/s. The retention window is about 8 min.

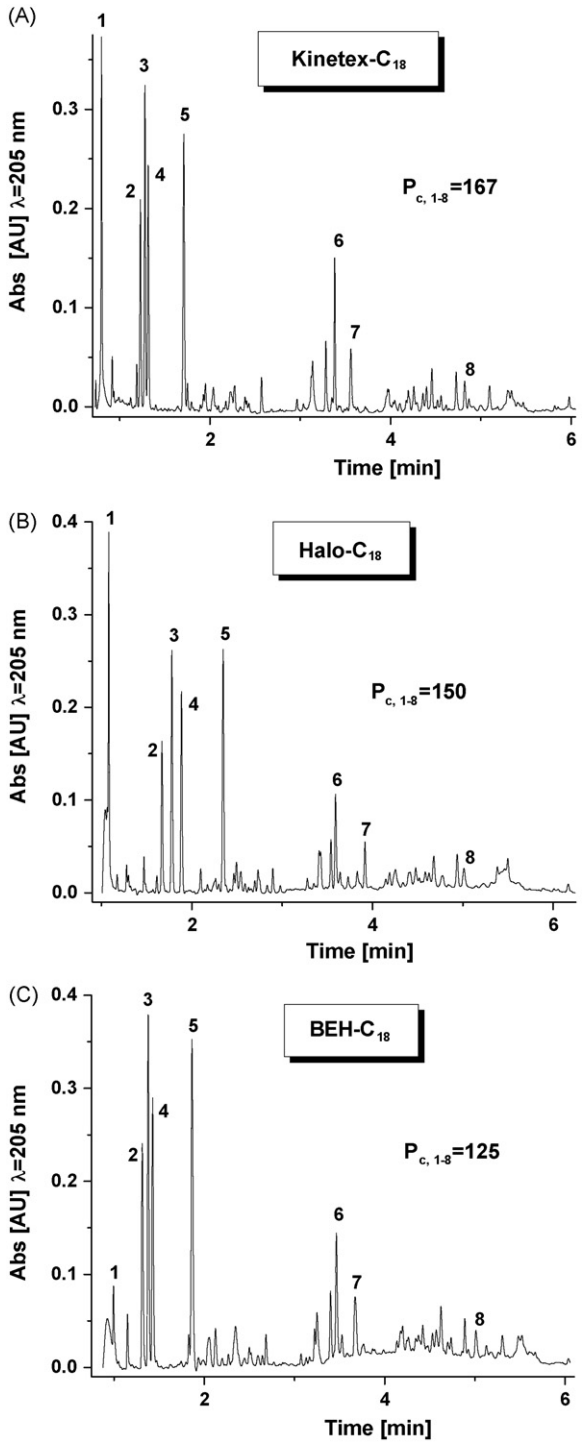

Fig. 4. Same as in Fig. 2 except the linear velocity was set at 0.370 cm/s. The retention window is about 4 min.

explained by the heat friction effects outweighing the increase of plate height when the mobile phase velocity and the inlet pressure increase. It could also be caused by a larger stagnant C term of the BEH column when increasing the linear velocity. Actually, at constant u_0, the column pressure drop of the sub-2 μm BEH column is more than 1.5 times larger than that of the 2.6 μm Kinetex column, which has the same length, 10 cm. Table 1 reports the specific permeability k_0 of these two columns, 2.77×10^{-11} cm^2 (BEH) and 4.46×10^{-11} cm^2 (Kinetex), a ratio close to 1.6, in agreement with the pressure drops measured.

In the last column of Table 2 are listed the calculated values of the plate height that would give a perfect match between experimental (Fig. 1) and theoretical (Eq. (14)) peak capacities. Although a single H value has no real physical meaning because a large collection of peptides is analyzed and the HETP depends on the mobile phase composition [22,23], this number is a strong indicator of the column performance. At constant intrinsic gradient steepness and column length, the lower H, the better the column performance in gradient elution. Table 2 provides three important conclusions. We observe first that H is minimum for an intermediate velocity for both the Halo and the Kinetex columns (closer to the minimum HETP).

Second, for all columns, H slightly increases with increasing gradient steepness. Although fast gradients are desired to decrease the analysis time, too steep gradient slopes affect negatively the peak capacity. At any linear velocity and with $G \simeq 10$, one cannot achieve a peak capacity better than about 85–90% of the peak capacity reached with $G \simeq 1$, possibly because Eq. (14) could overestimate the peak compression of peptides at high gradient steepness. Also, it was shown experimentally that the optimum range of gradient

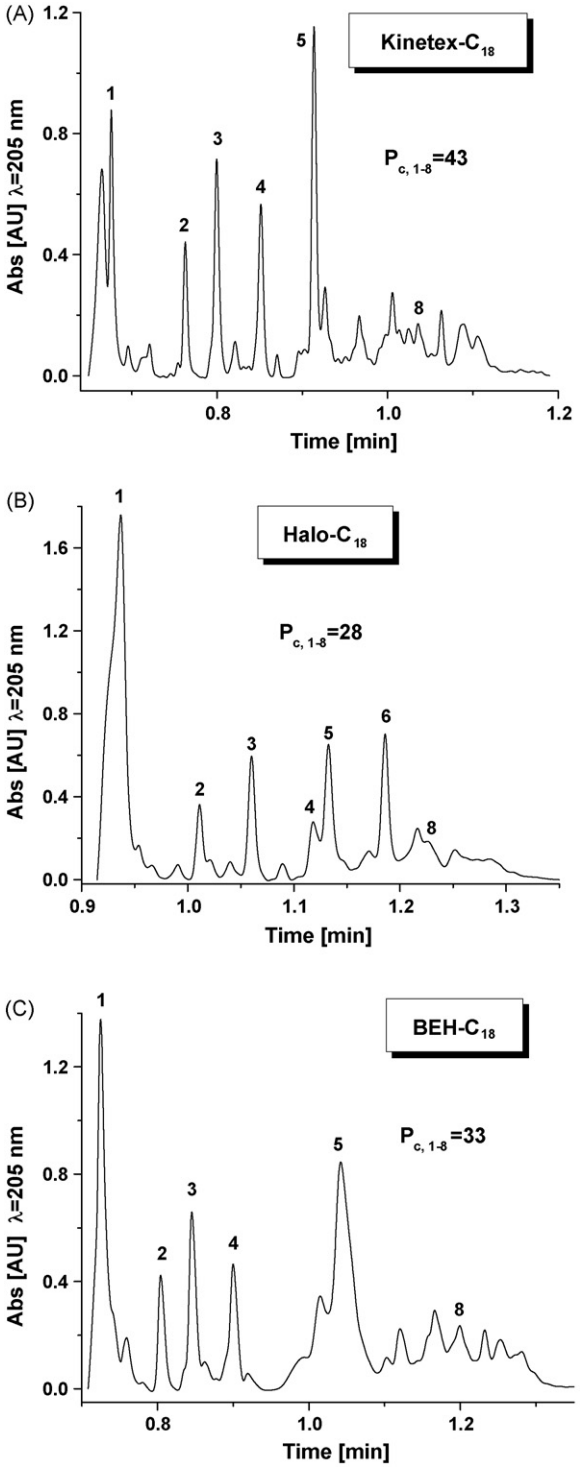

Fig. 5. Same as in Fig. 2 except the linear velocity was set at 0.370 cm/s and the gradient slope β/u_0 was maximum at 2.25 m^{-1}. The retention window is about 0.4 min (24 s). Note the better peak capacity of Kinetex illustrated from the resolution of the smallest peaks along the baseline.

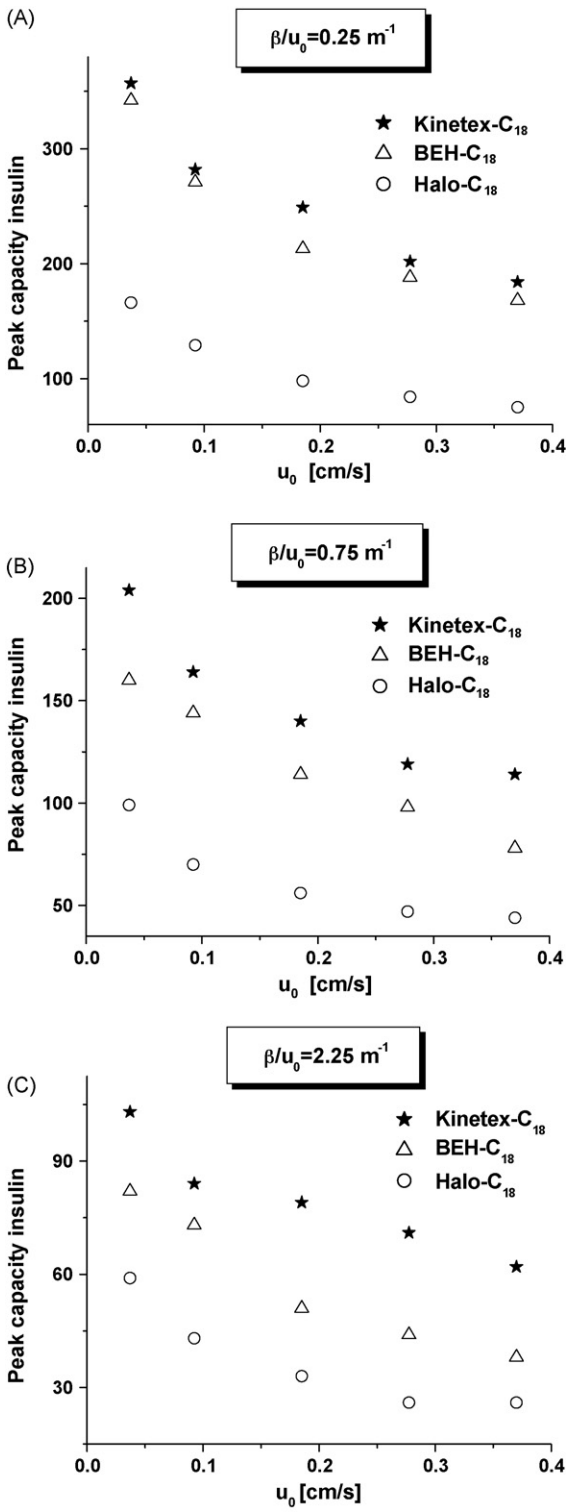

Fig. 6. Comparison between the peak capacities measured from the peakwidth of the protein insulin as a function of the linear velocity u_0 on the 100 mm × 4.6 mm 2.6 μm Kinetex-C_{18}, 150 mm × 4.6 mm 2.7 μm Halo-C_{18}, and 100 mm × 3.0 mm 1.7 μm BEH-C_{18} columns. The retention window was measured as the difference between the elution times of the last eluted protein, lyzozyme, and that of a small non-retained molecule, thiourea. Three gradient slopes $\frac{\beta}{u_0}$ were applied: (A) 0.25 m^{-1}, (B) 0.75 m^{-1}, and (C) 2.25 m^{-1}. In contrast to Fig. 1 (where the peak bandwidth of peptides were measured), note the significant decrease of the peak capacity as the flow rate in increased.

steepness is around 0.1 for peptides [17]. Our results are consistent with this finding. Finally, despite being packed with smaller particles, the BEH column exhibits H values which are comparable at low linear velocity and low gradient steepness to those exhibited by the Halo and Kinetex columns. In contrast, H is significantly larger at high velocities and high gradient steepness. For instance, the peak capacity of the BEH column measured at $G = 8.34$, for $u_0 = 0.37$ cm/s is only 75% of the peak capacity measured with the Kinetex column. We would rather have expected the opposite behavior since small particles should provide lower plate height H. A possible explanation could be due to the heat friction released at high flow rates. The heat power friction released in the BEH column per volume unit is typically twice larger than that released in the Kinetex column [31]. However, because the diameter of the BEH column is only 3.0 mm *versus* 4.6 mm for the Kinetex column, the temperature difference between the center and the wall of these two columns may not be significantly different. Only precise numerical calculations [32] will eventually show the difference. This would require a large amount of data such as the axial temperature profile of the external tube and the effect of temperature and pressure on the density, viscosity, and heat conductivity of the eluent. Still, heat effects are present and may cause significant apparent efficiency losses when a sub-2 μm BEH column is operated at high gradient speed and high gradient steepness. At the highest linear velocity, the heat power friction is of the order of 10 W/m, a value clearly larger than 4 W/m above which the columns start losing efficiency due to the formation of radial temperature gradients [33,11]. Assuming a linear gradient, a LSS retention model, an ideal inlet flow distributor, an homogeneous packed bed structure, and a constant wall temperature ($T = T_W$), the difference between the retention factors expected at the column outlet ($z = L$) between the column center and its wall is approximately given by [22]:

$$\frac{\Delta k'}{k'} \simeq GB \ln 10 \frac{T_C - T_W}{T_W^2} \tag{20}$$

where B is a constant that depends on the viscosity of the mobile phase ($B = 386$ K for pure acetonitrile) and $T_C > T_W$ is the temperature at the column center, larger than the temperature of the wall T_W, due to heat friction. Thus, we expect that the higher the intrinsic gradient steepness G, the larger the difference between the retention factors of any compound in the column center and close to its wall, hence the larger the loss of column efficiency. Note that Eq. (20) accounts only for the radial distribution of both the composition and the viscosity of the mobile phase across the column diameter in linear gradient elution. It ignores the effect of the temperature on the retention of the sample. The relative difference in the retention factors taken in the center and at the wall of the column given by Eq. (20) is then a minimum.

We also observe that the performance of the Halo column is significantly lower than that of the Kinetex column for the fastest and steepest gradients (−35%). The Halo column has a larger C term than the Kinetex column, as was demonstrated earlier under isocratic conditions [12]. This may well explain the differences observed between the performance of the two columns during the gradient elution of a large collection of peptides. However, it is noteworthy that the gradient steepness G of the Halo column are experimentally steeper that those of the Kinetex columns (see Table 2) because these two columns have different lengths, 15 and 10 cm, respectively. So, the results may be biased and the performance difference between the two columns be overestimated. In order to avoid this bias, we recalculated the theoretical peak capacities for an hypothetical 10 cm long Halo column. Then, the gradient steepness is the same for both columns. The calculations showed that decreasing the column length from 15 to 10 cm lead to a 12% increase of

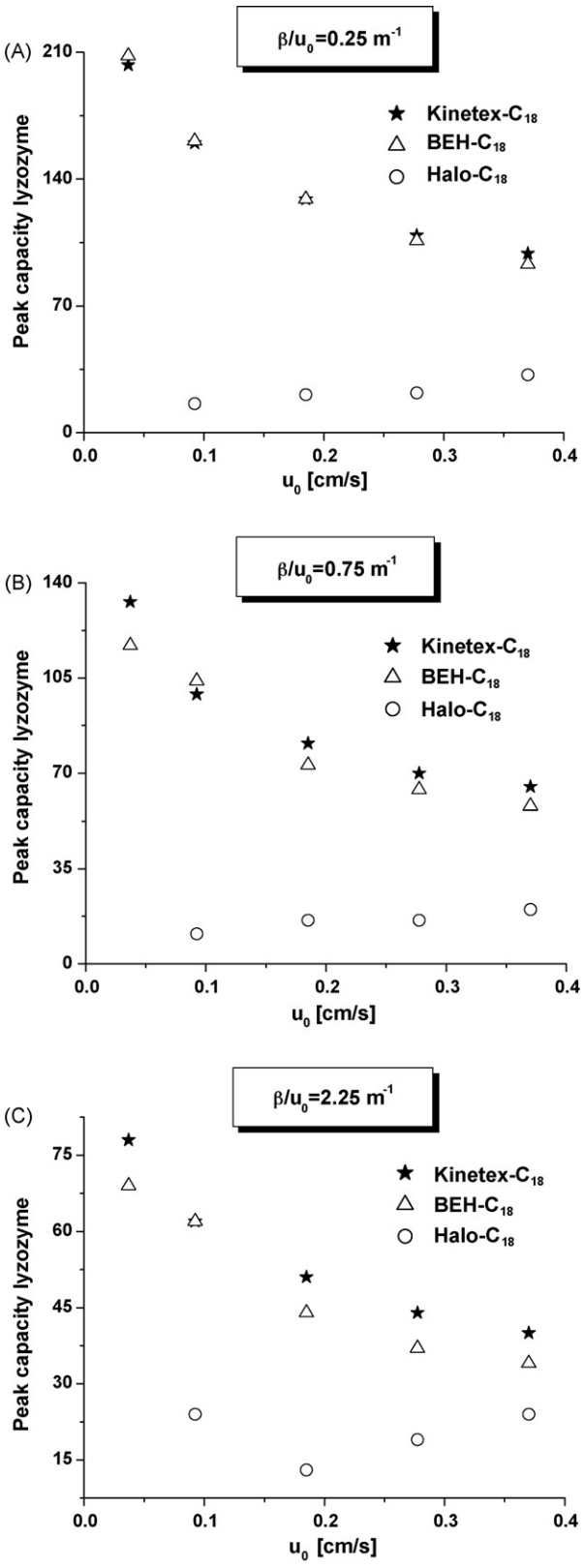

Fig. 7. Same as in Fig. 6, except the peak capacities were measured from the peak-width of the last eluted protein, lyzozyme. Note the comparable performances of the 2.6 μm Kinetex-C_{18} shell particles and 1.7 μm BEH-C_{18} totally porous particles and the failure of the Halo column to elute properly lyzozyme (see Fig. 8).

the peak capacity at $G = 8.34$. Accordingly, the performance of the Halo column at high flow rates and high gradient steepness reaches 75–80% of the performance of the Kinetex column.

In summary, the Halo-C_{18} and the BEH-C_{18} columns have similar performance while the Kinetex-C_{18} column yields separations which exhibit a peak capacity about 20% higher than those of the other two columns at high gradient speeds. This conclusion is illustrated in Fig. 5A–C which compares the separations of the β-lactoglobulin digest at a maximum linear velocity of 0.37 cm/s and at the steepest intrinsic gradient steepness of about 10. We observe that the peaks are homogeneously resolved across the gradient window (0.4 min) with the Kinetex column (back pressure ca. 540 bar). In contrast, the Halo column cannot satisfactorily resolve the most retained peptides, those that are the most hydrophobic and voluminous. The Halo column (back pressure ca. 580 bar) seems to experience limitations regarding the mass transfer of large peptides, as previously reported with the small protein insulin [12,34]. The resolution given by the BEH column (back pressure ca. 815 bar) is homogeneous across the retention window but it is less than that afforded by the Kinetex column because the BEH column back pressure is higher, frictional heating effects are more important and decrease the column efficiency, especially at high gradient steepness (see Eq. (20)).

4.2. Peak capacity for a mixture of two proteins: insulin and lyzozyme

In this series of experiment, five different linear velocities were applied (0.037, 0.093, 0.185, 0.28, and 0.370 cm/s). Two different peak capacities were measured, one based on the peak width of insulin, the other on that of lysozyme. In both cases, the retention window was taken as the difference between the elution times of lysozyme and thiourea. The results are shown in Fig. 6 (peak capacity based on the peak width of insulin) and in Fig. 7 (peak capacity based on the peak width of lysozyme).

In contrast to what was observed with the peptide mixture studied in the previous section, the peak capacities decrease clearly with increasing linear velocity. Despite the constancy of the intrinsic gradient steepness from one flow rate to the next, all three columns are losing about 50% of their initial peak capacity as the flow rate is increased 10-fold. This loss of peak capacity is directly related to the increase of the HETP of the proteins with increasing linear

Table 3
Experimental flow rates, gradient times, and gradient steepnesses applied on the Kinetex, Halo, and BEH columns for the analysis of the proteins insulin (MW = 5800 with $S{\sim}68$) and lyzozyme (MW = 14, 300 with $S{\sim}105$). The increase in the concentration of acetonitrile is maintained constant at $\Delta\varphi = 0.40$. H is the average column plate height which allows matching experimental and theoretical peak capacities (Eq. (14)).

Column	F_v (mL/min)	u_0 (cm/s)	t_g (min)	$G = S\beta t_{0Insulin}$	$H_{Insulin}$ (μm)	$G = S\beta t_{0Lyzozyme}$	$H_{Lyzozyme}$ (μm)	$H_{Lyzozyme}/d_p$
	0.200	0.037	63.0	1.63	4.3	2.46	19.0	7.3
			21.0	4.88	3.5	7.37	9.9	3.8
			7.0	14.63	2.3	22.11	4.3	1.7
	0.500	0.093	25.2	1.62	6.9	2.43	30.7	11.8
			8.4	4.87	5.5	7.30	18.0	6.9
			2.8	14.61	3.5	21.90	7.5	2.9
Kinetex-C_{18} 100 mm × 4.6 mm	1.000	0.185	12.6	1.62	8.9	2.45	46.6	17.9
			4.2	4.87	7.5	7.35	26.4	10.2
			1.4	14.60	4.1	22.06	10.9	4.2
	1.500	0.278	8.4	1.63	14.7	2.42	64.9	25.0
			2.8	4.88	13.7	7.27	37.8	14.5
			0.9	14.64	5.1	21.81	14.2	5.5
	2.000	0.370	6.3	1.63	16.8	2.41	79.3	30.5
			2.1	4.89	11.7	7.23	41.1	15.8
			0.7	14.67	6.8	21.69	16.3	6.3
	0.196	0.037	63.0	2.72	18.7	n.a.	n.a.	n.a.
			21.0	8.17	10.7	n.a.	n.a.	n.a.
			7.0	24.50	4.4	n.a.	n.a.	n.a.
	0.491	0.093	25.2	2.73	30.8	5.16	2102	778.5
			8.4	8.19	21.7	15.48	714	264.4
			2.8	24.58	8.6	46.44	33	12.2
Halo-C_{18} 150 mm × 4.6 mm	0.982	0.185	12.6	2.74	54.7	5.10	2016	746.7
			4.2	8.21	34.7	15.30	546	202.2
			1.4	24.62	14.9	45.91	608	225.2
	1.472	0.278	8.4	2.74	72.2	5.19	1944	720.0
			2.8	8.21	47.3	15.58	520	192.6
			0.9	24.62	24.0	46.73	49	18.1
	1.963	0.370	6.3	2.72	91.7	5.28	1799	666.3
			2.1	8.17	55.4	15.84	356	131.9
			0.7	24.50	23.7	47.51	29	10.7
	0.103	0.037	63.0	1.68	4.7	2.20	16.3	9.6
			21.0	5.04	5.8	6.59	12.0	7.1
			7.0	15.13	3.7	19.78	5.6	3.3
	0.257	0.093	12.6	1.68	7.7	2.18	27.8	16.4
			4.2	5.03	7.2	6.53	15.6	9.2
			1.4	15.08	4.8	19.58	7.0	4.1
BEH-C_{18} 100 mm × 3.0 mm	0.513	0.185	6.3	1.68	12.8	2.16	43.7	25.7
			2.1	5.03	11.7	6.47	32.2	18.9
			0.7	15.08	10.1	19.41	14.4	8.5
	0.770	0.278	63.0	1.66	16.8	2.11	66.6	39.2
			21.0	4.99	16.4	6.33	43.8	25.8
			7.0	14.97	14.6	19.00	21.5	12.6
	1.026	0.370	12.6	1.66	21.4	2.09	87.1	51.2
			4.2	4.97	26.4	6.28	54.4	32.0
			1.4	14.90	19.9	18.85	25.7	15.1

velocity, due to their relatively slow diffusion from the stream of eluent percolating the bed to the eluent stagnant in the porous stationary phase and through these particles. According to Eq. (14), H increases approximately four times when u_0 increases from 0.037 to 0.370 cm/s. Table 3 lists the H values that allow matching the experimental and theoretical peak capacities for different velocities. A similar behavior was not observed with the peptide mixture because the HETP for peptides is barely affected by an increase of the linear velocity [12].

An interesting finding is that the HETP of insulin and lysozyme systematically decreases with increasing intrinsic gradient steepness at constant linear velocity. It decreases with insulin by about 50, 70, and 20% on the Kinetex, the Halo, and the BEH columns, respectively. This decrease is more important for lyzozyme, 80 and 70% on the Kinetex and the BEH columns, respectively. This behavior is the opposite of what is observed with the peptides of the β-lactoglobulin digest, in which case H increases by about 40, 100, and 60% for these same three columns, respectively. This means that, when the intrinsic gradient steepness increases, the band compression factors of the peptides and the proteins are overestimated and underestimated, respectively. These compression factors were derived using the approach of Poppe et al. [26] and Eq. (3) that was introduced in the model of peak capacity of Eq. (14). A more general expression of the peak compression factor of proteins is needed. Its development requires the measurement of the retention factors and column plate heights at various mobile phase compositions under isocratic conditions [23].

The Kinetex and BEH columns behave similarly, despite the fact that the average mesopore size of the BEH particles (130 Å) is significantly larger than that of the Kinetex particles (96 Å). This proves that the mass transfer of insulin and lyzozyme through the 0.35 μm porous shell of the Kinetex particles is about as fast as that through the totally porous 1.7 μm BEH particles. This rapid mass transfer of proteins through the porous shell of the Kinetex particles is certainly due to (1) the reduced average path length across the porous medium, which speeds up diffusion and reduces the duration of the mass transfer by a factor 2.3 by respect to that needed in a totally porous particles [13]; and (2) the ordered structure of the porous shell that is made of 10 successive thin layers of fine silica particles [12]. In theory, assuming the same sample diffusivity coefficient through both the Kinetex porous shell and the BEH porous particles, one would expect that the ratio of their C terms be of the order of $C_{Kinetex}/C_{BEH} = d^2_{p,Kinetex}/2.3d^2_{p,BEH} = 2.6^2/2.3 \times 1.7^2 = 1.02$ [12,13]. In addition, the average pore size of the BEH particles is larger than that of the Kinetex particles and their internal porosity ϵ_p are comparable (0.436 *versus* 0.444) so we might reasonably have expected a larger sample diffusivity through the BEH particles. According to the Renkin equation, we can estimate the hindrance diffusion factor of the proteins as follows:

$$F(\lambda_m) = (1-\lambda_m)^2(1 - 2.1044\lambda_m^2 + 2.089\lambda_m^3 - 0.948\lambda_m^5) \qquad (21)$$

where λ_m is the ratio of the molecular size of the protein to the average mesopore size of the porous shell. The sizes of insulin and lyzozyme are 32 and 42 Å, respectively [35]. After C_{18} derivatization of the silica surface, and for a surface coverage of 3 μmol/m^2, the decrease in average pore size is close to 20% [36]. Accordingly, the hindrance diffusion factors $F(\lambda_m)$ are 1.6 (insulin) and 2.0 (lyzozyme) times larger within the BEH porous particles than through the porous shell of the Kinetex particles. Actually, according to the values of H given in Table 3, the Kinetex column is not less efficient than the BEH column under gradient conditions. This explains why the C term of the Kinetex particles is so low, as was previously observed under isocratic conditions for both insulin and lyzozyme [12].

Strikingly, the peak capacities measured with the Halo column for the gradient elution separation of proteins are significantly lower than those observed on either of the other two columns The peak capacities decrease by about 50% for insulin and still more for lyzozyme. The very poor peak shape of lyzozyme could possibly be due to the combination of some secondary interactions

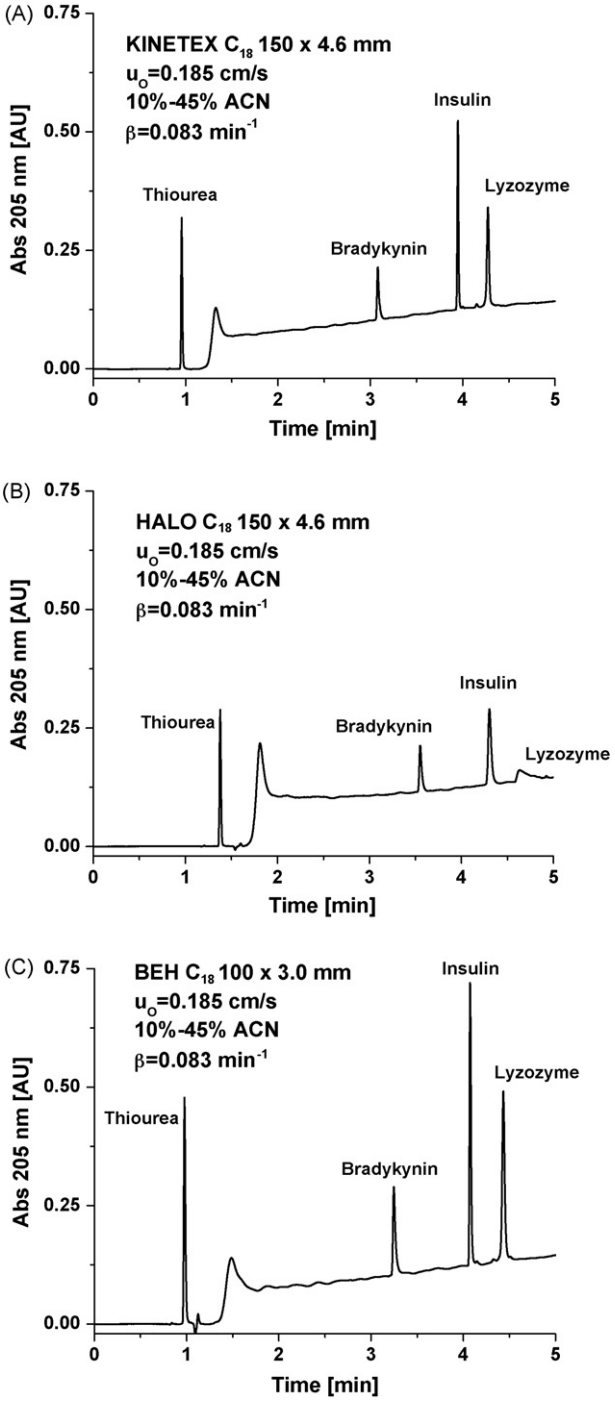

Fig. 8. Chromatograms obtained after the injection of 5 μL of a mixture of thiourea (non-retained marker), bradykinin (0.09 g/L), insulin (0.27 g/L), and lyzozyme (0.26 g/L) in gradient elution. The concentration of acetonitrile at the beginning and at the end of the gradient is equal to 10% and 45%, respectively. The flow rate was set so that the linear velocity u_0 was constant for all three columns at 0.185 cm/s. The gradient slope is maintained constant at $\beta/u_0 = 0.75\,m^{-1}$. The retention window ($t_{Lyzozyme} - t_{Thiourea}$) is about 4.5 min. T = 295 K. (A) 100 mm × 4.6 mm 2.6 μm Kinetex-C_{18} column, (B) 150 mm × 4.6 mm 2.7 μm Halo-C_{18} column, and (C) 100 mm × 3.0 mm 1.7 μm BEH-C_{18} column.

with the Halo particles, a large stagnant C term, and a strong diffusion hindrance in the Halo shells. Yet, there is no definitive answer in the literature. The manufacturer of Halo particles has always warned analysts of this limitation. Our model suggests that the ratio of the C terms of the Halo and the Kinetex columns particles should be $C_{Halo}/C_{Kinetex} = 2.3 \times d^2_{p,Halo}/1.7 \times d^2_{p,Kinetex} = 2.3 \times 2.7^2/1.7 \times 2.6^2 = 1.46$. However, Table 2 shows that, for insulin, the best HETP values estimated for the Halo column are 3–5 times larger than those obtained with the Kinetex column. Fig. 8 compares the performance of the Kinetex, the Halo, and the BEH column at the same linear velocity, u_0=0.185 cm/s and for the same gradient slope $\beta/u_0 = 0.75\,m^{-1}$. In the case of lyzozyme, the Halo column behaves so poorly that a comparison between the two columns does not make much sense. For reasons not yet clearly understood, the mass transfer of proteins with molecular masses larger than ca. 5 kDa is surprisingly slow with the Halo particles. This problem does not seem to be mainly caused by the small average pore size of the particles (90 Å) that causes a significant hindrance to diffusion through the mesopore network but possibly also, due to their rough and irregular external surface area that could cause slow external mass transfer and/or second interactions with the Halo-C_{18} particles.

5. Conclusion

Our results confirm the excellent performance of the new brand of columns packed with shell particles, the 2.6 μm Kinetex-C_{18}, under gradient elution. For the separation of the peptides in protein digests (β-lactoglobulin digest), the peak capacity of this column is similar to those of the 2.7 μm Halo shell particles and the 1.7 μm BEH totally porous particles at small reduced linear velocity ($\nu < 2$) and small intrinsic gradient steepness ($G < 1$). However, the Kinetex column maintains 100% of its performance at increasing flow velocities of the eluent. It provides peak capacities around 170 within four minutes, for a gradient steepness $G \simeq 1$ while peak capacities of only 150 and 125 are generated by the Halo and the BEH columns, respectively.

For the separation of authentic proteins by gradient elution, the peak capacities of all three columns significantly decrease with increasing the gradient slope at constant gradient steepness. This observation is due to the slow mass transfer kinetics of proteins through the porous shell and the porous particles. The performance of the Kinetex column is slightly better than that of the BEH column when the peak capacity is derived from the peakwidth of insulin but it is comparable when it is derived from the peakwidth of lyzozyme. This observations show the advantage of using shell particles to separate large biomolecules, because their intraparticle diffusivity is less than a few percent of their bulk diffusivity under non-retained conditions. The Kinetex column can provide a peak capacity of 85 with proteins of molecular mass around 15 kDa within three and a half minutes at a gradient steepness $G \simeq 6$ while the BEH and the Halo columns can only generate peak capacities of 75 and 15, respectively.

Acknowledgements

This work was supported in part by grant CHE-06-08659 of the National Science Foundation and by the cooperative agreement between the University of Tennessee and the Oak Ridge National Laboratory. We thank Tivadar Farkas (Phenomenex, Torrance, USA) and Uwe Dieter Neue (Waters, Milford, USA) for the generous gift of the Kinetex and BEH columns used in this work and for fruitful discussions.

References

[1] K. Nakanishi, N. Soga, J. Am. Ceram. Soc. 74 (1991) 2518.
[2] H. Minakuchi, K. Nakanishi, N. Soga, N. Ishizuka, N. Tanaka, Anal. Chem. 68 (1996) 3498.
[3] K. Cabrera, G. Wieland, D. Lubda, K. Nakanishi, N. Soga, H. Minakuchi, K.K. Unger, Trends Anal. Chem. 17 (1998) 133.
[4] 32nd International Symposium on High Performance Liquid Phase Separations and Related Techniques, Baltimore, MD, May 2008.
[5] Pittcon Conference & Expo 2009, Chicago, IL, March 8–13, 2009.
[6] J.J. Kirkland, Anal. Chem. 41 (1969) 218.
[7] J.J. DeStefano, T.J. Langlois, J.J. Kirkland, J. Chromatogr. Sci. 46 (2007) 254–260.
[8] F. Gritti, G. Guiochon, J. Chromatogr. A 1169 (2007) 125.
[9] A. Cavazzini, F. Gritti, K. Kaczmarski, G. Guiochon, Anal. Chem. 79 (2007) 5972.
[10] 34th International Symposium on High Performance Liquid Phase Separations and Related Techniques (HPLC-2009), Dresden, Germany.
[11] F. Gritti, G. Guiochon, J. Chromatogr. A 1216 (2009) 1353.
[12] F. Gritti, I. Leonardis, D. Shock, P. Stevenson, A. Shalliker, G. Guiochon, J. Chromatogr. A 1217 (2010) 1589–1603.
[13] K. Kaczmarski, G. Guiochon, Anal. Chem. 79 (2007) 4648.
[14] J.J. Kirkland, Anal. Chem. 64 (1992) 1239.
[15] J.J. Kirkland, F.A. Truszkowski, C.H. Dilks, G.S. Engel Jr., J. Chromatogr. A 890 (2000) 3.
[16] J.H. Knox, J. Vasvari, J. Chromatogr. 83 (1973) 181.
[17] X. Wang, D.R. Stoll, A. Schellinger, P.W. Carr, Anal. Chem. 78 (2006) 3406.
[18] F. Gritti, G. Guiochon, J. Chromatogr. A 1157 (2007) 289.
[19] C. Dewaele, M. Verzele, J. Chromatogr. 260 (1983) 13.
[20] G. Carta, J.S. Bauer, AIChE J. 36 (1990) 147.
[21] J. Abia, K. Mriziq, G. Guiochon, J. Chromatogr. A 1216 (2009) 3185.
[22] F. Gritti, G. Guiochon, J. Chromatogr. A 1215 (2008) 64.
[23] F. Gritti, G. Guiochon, J. Chromatogr. A 1216 (2009) 6124.
[24] U.D. Neue, J. Chromatogr. A 1079 (2005) 153.
[25] F. Gritti, G. Guiochon, J. Chromatogr. A 1145 (2007) 67.
[26] H. Poppe, J. Paanaker, M. Bronckhorst, J. Chromatogr. 204 (1981) 77.
[27] L. Snyder, High Performance Liquid Chromatography – Advances and Perspectives, Elsevier, Amsterdam, 1986, p. 10.
[28] M. Gilar, A.E. Daly, M. Kele, U.D. Neue, J.C. Gebler, J. Chromatogr. A 1061 (2004) 183.
[29] J. Giddings, Dynamics of Chromatography, Marcel Dekker, New York, NY, 1965.
[30] N. Marchetti, A. Cavazzini, F. Gritti, G. Guiochon, J. Chromatogr. A 1163 (2007) 203.
[31] H. Lin, C. Horváth, Chem. Eng. Sci. 36 (1981) 47.
[32] K. Kaczmarski, F. Gritti, J. Kotska, G. Guiochon, J. Chromatogr. A 1216 (2009) 6575.
[33] F. Gritti, G. Guiochon, Anal. Chem. 80 (2008) 5009.
[34] F. Gritti, G. Guiochon, J. Chromatogr. A 1166 (2007) 30.
[35] F. Gritti, G. Guiochon, J. Chromatogr. A 1176 (2007) 107.
[36] F. Gritti, G. Guiochon, Anal. Chem. 78 (2006) 5329.